Dynamic deformation of the accretionary prism excites very low frequency earthquakes

著者	Ito Yoshihiro, Obara Kazushige
journal or publication title	Geophysical Research Letters
volume	33
page range	L02311
year	2006
URL	http://hdl.handle.net/10097/51465

doi: 10.1029/2005GL025270

Dynamic deformation of the accretionary prism excites very low frequency earthquakes

Yoshihiro Ito and Kazushige Obara
National Research Institute for Earth Science and Disaster Prevention, Tsukuba, Japan

Received 19 November 2005; accepted 20 December 2005; published 25 January 2006.

[1] We have detected anomalous very-low-frequency earthquakes within the accretionary prism along the Nankai Trough, southwestern Japan. Centroid moment tensor inversion analysis reveals that the earthquake hypocenters are distributed at ~10 km depth above the upper surface of the subducting Philippine Sea Plate, and within 50–70 km landward of the trough axis. The focal mechanisms indicate reverse faulting. Their hypocenters are distributed beneath a deformation zone of an accretionary prism in sea-floor topography. These observations suggest that the occurrence of very-low-frequency earthquakes is related to numerous reverse fault systems within the accretionary prism, and that the earthquakes reflect the dynamics of deformation within this accretionary prism.
Citation: Ito, Y., and K. Obara (2006), Dynamic deformation of the accretionary prism excites very low frequency earthquakes, *Geophys. Res. Lett.*, *33*, L02311, doi:10.1029/2005GL025270.

1. Introduction

[2] The Nankai Trough represents the deformation front of the subduction zone where the Philippine Sea Plate subducts beneath the margin of the Eurasian Plate at the rate of ~4 cm/yr [*Seno et al.*, 1993] (Figure 1a). The sediments that were scraped off the top of the subducting Philippine Sea Plate have formed a 5–10 km thick accretionary prism landward of the Nankai Trough. Megathrust earthquakes commonly occur along the plate boundary in this region. Therefore, an understanding of the deformation processes within the accretionary prism is important for monitoring the plate motion. A recent seismic profile revealed a well-developed reverse fault system within the accretionary prism above the decollement [e.g., *Moore et al.*, 1990; *Park et al.*, 2002]. No evidence of seismic activity has previously been documented within the accretionary prism, although the development of reverse faults indicates the shortening of the prism.

[3] Anomalous very-low-frequency (VLF) earthquakes are observed near the trench axis along the Nankai Trough [*Ishihara*, 2003]. VLF earthquakes along the Nankai Trough have a predominant period range of 10–20 s [*Obara and Ito*, 2005]. These earthquakes have not been described in any earthquake catalog because they have no distinct short period phases of a *P* or *S* wave component [see *Obara and Ito*, 2005, Figure 8]. The low-frequency wave trains are composed of surface waves with an apparent velocity of around 3.8 km/s, and the earthquake epicenters are located landward of the Nankai Trough, as estimated from the directions of the wave train propagation [*Obara and Ito*, 2005]. However, their accurate source locations and fault models have not been revealed thus far.

[4] In this study, we apply the centroid moment tensor (CMT) inversion method to the waveform of VLF earthquakes that are observed by the densely distributed seismic network established by the National Research Institute for Earth Science and Disaster Prevention (NIED). We propose a source model for VLF earthquakes by analyzing the source locations and focal mechanisms of VLF earthquakes.

2. Method and Data

[5] We adopted the CMT inversion method [*Ito et al.*, 2005] to calculate the moment tensor solutions, centroid locations, and centroid times. In this method, the centroid locations and times with maximum variance reduction were calculated by a grid-search algorithm. The calculated grid-points were arranged around an initial epicenter estimated by cross-correlation analysis [*Obara and Ito*, 2005]. The horizontal and vertical grid intervals were 1 km and spanned 1 s in time. The algorithm for calculating the moment tensor solution at each grid-point was based on a standard waveform inversion technique [e.g., *Dreger and Helmberger*, 1993]. The source location and origin time were determined by using a grid-search algorithm that determined the best moment tensor solution. In order to calculate Green's functions, we employed the same velocity and seismic attenuation model as that for the routine NIED F-net moment tensor analysis [*Fukuyama et al.*, 1998].

[6] We used the waveform observed from the NIED broadband velocity seismometer network (F-net) and high sensitive accelerometer network (Hi-net TILT) [*Okada et al.*, 2004; *Obara et al.*, 2004] (Figure 1a). The NIED seismic network comprises ~650 Hi-net and ~70 F-net stations installed throughout Japan; it can detect a variety of movements such as non-volcanic deep tremors and short period slow slip events [*Obara*, 2002; *Obara et al.*, 2004]. Two horizontal components of high-sensitivity accelerometers within the Hi-net TILT network are used as tiltmeters; these are useful for detecting and analyzing long period events and provide the means of investigating very small amplitude and long period waveforms [*Obara and Ito*, 2005]. Two or three component seismograms of the NIED Hi-net TILT or F-net networks were integrated to determine displacement; they were then filtered over a 20–50 s period. The moment tensor solutions were calculated using full waveforms, including all phases, i.e., *P* wave, *S* wave, and surface waves, with a time window of 200 s from an origin time. We used waveform

0094-8276/06/2005GL025270$05.00

data observed at more than 20 stations in the CMT inversion method.

3. Results

3.1. Centroid Locations

[7] We applied the CMT inversion method to 498 VLF earthquakes that occurred in 2003 and 2004; these earthquakes were detected by cross-correlation analysis [*Obara and Ito*, 2005]. We selected 27 moment tensor solutions if the variance reduction exceeded 50%. However, when the synthetic waveforms completely agree with observed ones, the variance reduction is 100%. The calculated VLF earthquakes had moment magnitudes in the range of M_W 3.6–4.4. Figure 2 shows an example of a calculated moment tensor solution of a VLF earthquake with a moment magnitude of 3.7 and a variance reduction of 70%. Synthetic waveforms of almost all stations were consistent with the observed ones. The observed and synthetic waveforms of four stations–MNMH, NKMH of NIED Hi-net TILT, KNMF and TGAF of F-net–are shown in Figure 2. The waveforms of MNMH and KNMF were examples of waveforms in good agreement. On the other hand, the waveforms of NKMH and TGAF were examples of mediocre and bad agreement for this event. However, in general the synthetic waveforms of four stations showed a good agreement with the observed ones. Figure 3 shows the centroid depths and moment tensor solutions as functions in variance reduction for two results with a variance reduction of 70% and 52%; the result with a variance reduction of 70% is the same event as that shown in Figure 2. Although the moment tensor solutions at the estimated depth did not differ from others obtained near the estimated depth, the variance reductions were decreased as the solutions showed an increasing disparity with the estimated depth. In particular, these features were highly prominent at deeper grids.

[8] VLF earthquakes, which were analyzed by the CMT method, generally occurred within 50–70 km landward of the trough axis and at a depth of ~10 km, above the upper surface of the subducting Philippine Sea Plate [*Sagiya and Thatcher*, 1999] (Figure 1a).

[9] In order to test the reliability of the locations estimated by the CMT inversion method, we applied the same method to determine the locations of 62 ordinary earthquakes of $M_W \sim 4$ that occurred in the study area; this was achieved by using the same seismic network and filter as those for

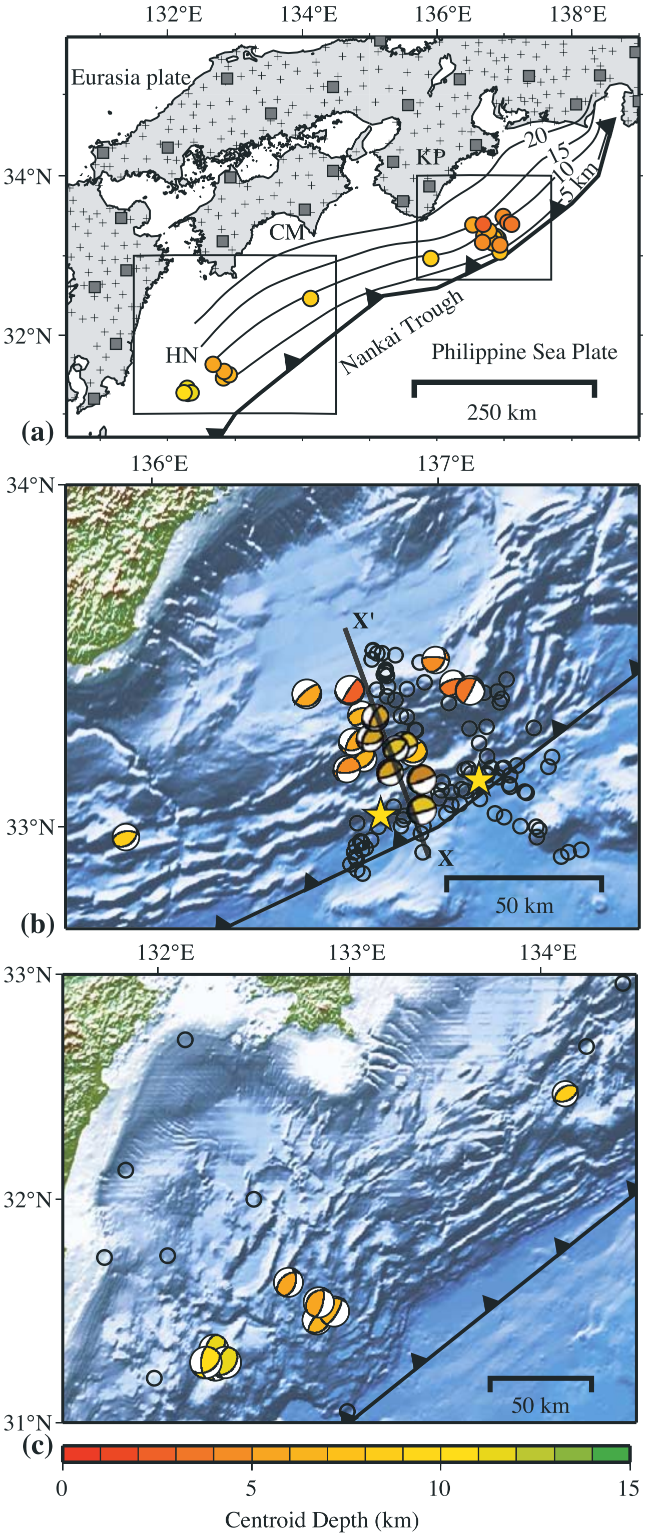

Figure 1. Hypocentral distribution of very-low-frequency (VLF) earthquakes during 2003 and 2004. (a) Tectonic setting, location of seismic stations, and VLF earthquake distribution. The circles represent the locations of VLF earthquakes. The crosses and squares represent the Hi-net and F-net stations, respectively. The color of the circle indicates the earthquake depth, as represented on the scale bar. The two rectangles indicate the areas shown in Figures 1b and 1c. The thick line with tick marks represents the axis of the Nankai Trough. The depth contours indicate the upper surface of the Philippine Sea Plate [*Sagiya and Thatcher*, 1999]. KP denotes the Kii peninsula; CM, Cape Muroto; and HN, Hyuga-nada (off Hyuga). (b) The region off the Kii peninsula. Focal spheres indicate the moment tensor solutions of the VLF earthquakes. The yellow stars represent intra-slab earthquakes of magnitudes greater than 7 that occurred on September 5, 2004 [*Ito et al.*, 2005]. The open circles indicate the locations of the aftershocks of magnitudes greater than 3.5. The line X–X′ marks the location of the cross section shown in Figure 4a. (c) The area off Cape Muroto and Hyuga-nada. The open circles indicate the locations of earthquakes of magnitude greater than 3.5 that occurred during 2003.

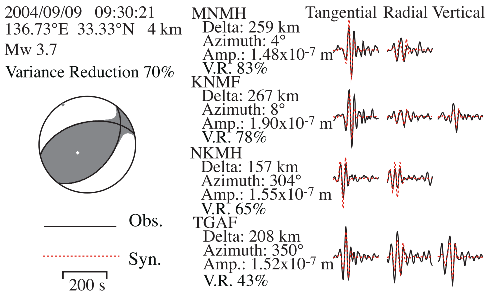

Figure 2. Example of the obtained moment tensor solutions and the observed and synthetic waveforms. The solid and red broken lines indicate the observed and synthetic waveforms, respectively.

VLF earthquakes. These events were related to two large earthquakes with a moment magnitude greater than 7 that occurred within the oceanic crust beneath the Nankai Trough on September 5, 2004 (Figure 1b). We compared the epicentral locations determined by the CMT inversion method with those determined by conventional hypocentral determination from the onset times of *P* and *S* waves. The horizontal deviations between the two approaches in determining the 62 events range from 0.4–28 km, with more than 85% of the differences being less than 5 km. The estimated depth distribution, at a depth of 5–20 km beneath the trough axis, was in good agreement with the estimates derived from an ocean-bottom seismometer network by *Sakai et al.* [2005].

3.2. Moment Tensor Solutions and Fault Planes

[10] All moment tensor solutions indicated reverse faulting. A small number of VLF earthquakes close to the trough axis yielded a nodal plane, which is one possible fault plane, coincident with the dip of the plate boundary. However, in the case of most VLF earthquakes, no nodal plane had an orientation similar to that of the plate boundary. The epicenters of the VLF earthquakes were distributed beneath a deformation zone along the Nankai Trough (Figures 1b and 1c). The accretionary prism is located landward of the trough axis and has a thickness of 5–10 km [*Moore et al.*, 1999; *Park et al.*, 2002; *Nakanishi et al.*, 2002a, 2002b]. The multichannel seismic reflection profiles exhibit a well-developed reverse fault system with landward-dipping faults [*Moore et al.*, 1990; *Park et al.*, 2002]. Assuming the nodal planes dipping landward as the source faults of VLF earthquakes, we compared the orientation of the fault strikes to the seafloor surface features in Figures 1b and 1c. In general, the strike of the nodal planes was generally subparallel to the trough axis; further, it varied with that of the sea-floor topography. Therefore, we concluded that the VLF earthquakes are associated with the dynamic deformation of the accretionary prism.

4. Discussion

[11] The subduction zone in the area southeast of the Kii peninsula has been studied intensively, and we can compare fault orientations across the trough axis based on the crustal structure estimated from the seismic velocity images of this area [*Nakanishi et al.*, 2002a] (Figure 4a). Most of the VLF earthquakes occurred within the sedimentary wedge of the accretionary prism between the trough axis and the outer ridge, which has a *P* wave velocity of 2–4 km/s; however, a few occurred within older accretionary sediments that have a *P* wave velocity greater than 5 km/s. The nodal planes dipping landward were observed to be steeper in the more landward areas. The same trend is observed for the Hyuga-nada region (Figure 4b). A decollement beneath the sedimentary wedge is parallel to the plate boundary and extends from the trough axis to the outer ridge. Many out-of-sequence thrusts (OST) branch upward from the decollement [*Moore et al.*, 1990] to the upper surface of the accretionary prism. A second type of thrust fault—a mega-splay fault—occurs in the more landward areas beneath the forearc basin. The mega-splay faults occur ∼55 km landward of the trough axis and branch out from the plate boundary at a depth of ∼10 km; the faults become steeper as they approach the sea floor in the vicinity of the outer ridge, near the Kii peninsula [*Park et al.*, 2002]. Due to the shortening of the accretionary prism, the VLF earthquakes may occur on OSTs or mega-splay faults that branch from the decollement or plate boundary (Figure 4c).

[12] The thrust faults generate a reverse-polarity reflection on seismic reflection profiles; this may indicate the existence of elevated fluid pressures within the fault zones [*Shipley et al.*, 1994] or that the fault zones are pathways of fluid migration [*Park et al.*, 2002]. The generation of VLF earthquakes may be related to the fluid within the fault zones and the low seismic velocity of the accretionary prism. High fluid pressure may weaken the fault through a reduction in the normal stress on the fault plane, and the resulting stick-slip behavior may produce low-stress-drop earthquakes in the zone of low seismic velocity. The VLF earthquakes near the Kii peninsula occurred following two large earthquakes of magnitude greater than 7, which occurred off the Kii peninsula [*Obara and Ito*, 2005]. The large earthquakes may have induced the migration of fluid along the existing faults or created new fractures, thereby triggering the VLF earthquakes.

5. Conclusion

[13] We determined the centroid moment tensors and locations of VLF earthquakes that occurred along the Nankai Trough, Japan, by the CMT inversion method. Their sources were located within the accretionary prism above the plate boundary between the Philippine Sea Plate and the Eurasian Plate, and within 50–70 km landward of the trough axis. The focal mechanisms revealed the occurrence of reverse faulting. We concluded that VLF earthquakes are

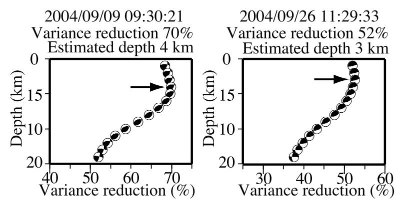

Figure 3. Two examples of variance reduction and moment tensor solutions plotted against the centroid depth. The arrows indicate the estimated depths in each event.

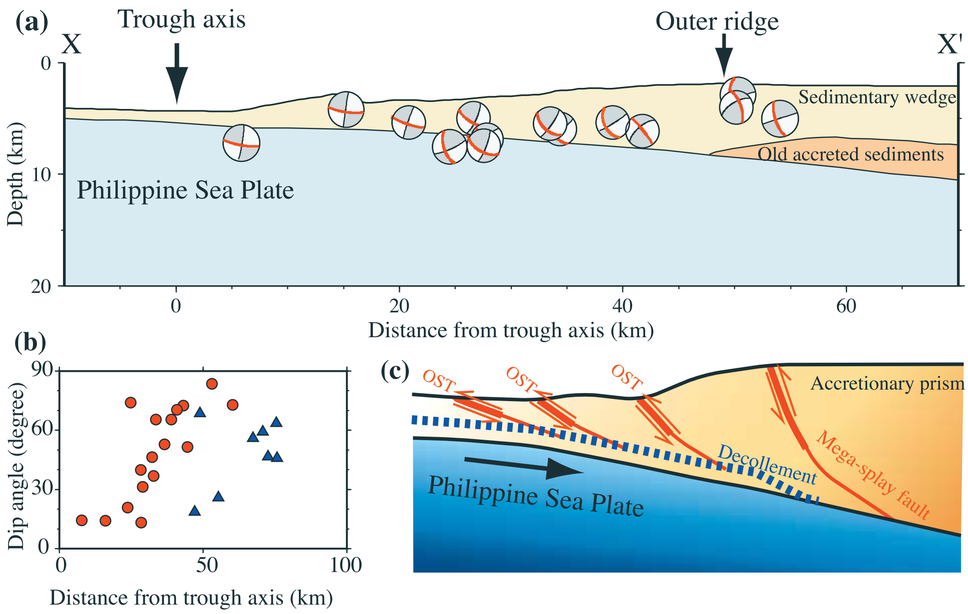

Figure 4. The crustal structure of the subduction zone and distribution of moment tensor solutions of VLF earthquakes. (a) The crustal structure determined from the seismic reflection profile [*Park et al.*, 2002] and wide-angle seismic survey [*Nakanishi et al.*, 2002a, 2002b]. The nodal planes dipping landward are colored in red. See Figure 1b for the location of the cross section X–X′. (b) The relationship between the distance from the trough axis and the dip of the fault planes. The red circles and blue triangles indicate events in the areas of the Kii peninsula and Hyuga-nada, respectively. (c) Schematic cross-section showing a source model for the VLF earthquakes. The red lines represent potential source faults for the VLF earthquakes including out-of-sequence thrusts (OST) [*Moore et al.*, 1990] and mega-splay faults [*Park et al.*, 2002]. The dotted blue line represents the decollement.

excited by the dynamic deformation of the accretionary prism.

[14] **Acknowledgments.** The article was significantly improved through constructive reviews by Goran Ekstrom and Kelin Wang. The Generic Mapping Tools (GMT) software [*Wessel and Smith*, 1991] was used to prepare the figures. We used bathymetrical data provided by the Japan Oceanographic Data Center.

References

Dreger, D. S., and D. V. Helmberger (1993), Determination of source parameters at regional distances with single station or sparse network data, *J. Geophys. Res.*, *98*, 8107–8125.

Fukuyama, E., M. Ishida, D. S. Dreger, and H. Kawai (1998), Automated seismic moment tensor determination by using on-line broadband seismic waveforms, *J. Seismol. Soc. Jpn.*, *51*, 149–156.

Ishihara, Y. (2003), Major existence of very low frequency earthquake in background seismicity along subduction zone of south-western Japan, *Eos Trans. AGU*, *84*(46), *Fall Meet Suppl.*, Abstract S41C-0107.

Ito, Y., T. Matsumoto, H. Kimura, H. Matsubayashi, K. Obara, and S. Sekiguchi (2005), Spatial distribution of centroid moment tensor solutions for the 2004 off Kii peninsula earthquakes, *Earth Planets Space*, *57*, 351–356.

Moore, G. F., T. H. Shipley, P. L. Stoffa, D. E. Karig, A. Taira, S. Kuramoto, H. Tokuyama, and K. Syuehiro (1990), Structure of the Nankai Trough accretionary zone from multichannel seismic reflection data, *J. Geophys. Res.*, *98*, 8753–8765.

Nakanishi, A., S. Kodaira, J. O. Park, and Y. Kaneda (2002a), Deformable backstop as seaward end of coseismic slip in the Nankai Trough seismogenic zone, *Earth Planet Sci. Lett.*, *203*, 255–263.

Nakanishi, A., N. Takahashi, J. O. Park, S. Miura, S. Kodaira, Y. Kaneda, N. Hirata, T. Iwasaki, and M. Nakamura (2002b), Crustal structure across the coseismic rupture zone of the 1994 Tonankai earthquake, the central Nankai Trough seismogenic zone, *J. Geophys. Res.*, *107*(B1), 2007, doi:10.1029/2001JB000424.

Obara, K. (2002), Nonvolcanic deep tremor associated with subduction in southwest Japan, *Science*, *296*, 1679–1681.

Obara, K., and Y. Ito (2005), Very low frequency earthquake excited by the 2004 off the Kii peninsula earthquake: A dynamic deformation process in the large accretionary prism, *Earth Planets Space*, *57*, 321–326.

Obara, K., H. Hirose, F. Yamamizu, and K. Kasahara (2004), Episodic slow slip events accompanied by non-volcanic tremors in southwest Japan subduction zone, *Geophys. Res. Lett.*, *31*, L23602, doi:10.1029/2004GL020848.

Okada, Y., K. Kasahara, S. Hori, K. Obara, S. Sekiguchi, H. Fujiwara, and A. Yamamoto (2004), Recent progress of seismic observation networks in Japan—Hi-net, F-net, K-NET, and KiK-net—, *Earth Planets Space*, *56*, xv–xxvii.

Park, J. O., T. Tsuru, S. Kodaira, P. R. Cummins, and Y. Kaneda (2002), Splay fault branching along the Nankai subduction zone, *Science*, *297*, 1157–1160.

Sagiya, T., and W. Thatcher (1999), Coseismic slip resolution along a plate boundary megathrust: The Nankai Trough, southwest Japan, *J. Geophys. Res.*, *104*, 1111–1129.

Sakai, S., T. Yamada, M. Shinohara, H. Hagiwara, T. Kanazawa, K. Obana, S. Kodaira, and Y. Kaneda (2005), Urgent aftershock observation of the 2004 off the Kii Peninsula earthquake using ocean bottom seismometers, *Earth Planets Space*, *57*, 363–368.

Seno, T., S. Stein, and A. E. Gripp (1993), A model for the motion of the Philippine Sea Plate consistent with NUVEL-1 and geological data, *J. Geophys. Res.*, *98*, 17,941–17,848.

Shipley, T. H., G. F. Moore, N. L. Bangs, J. C. Moore, and P. L. Stoffa (1994), Seismically inferred dilatancy distribution, northern Barbados ridge decollement; Implications for fluid migration and fault strength, *Geology*, *22*, 411–414.

Wessel, P., and W. H. F. Smith (1991), Free software helps map and display data, *Eos Trans. AGU*, *72*, 445–446.

Y. Ito and K. Obara, National Research Institute for Earth Science and Disaster Prevention, Tenno-dai 3-1, Tsukuba, Ibaraki 305-0006, Japan. (yito@bosai.go.jp)